Received: 7 February 2023 | Revised: 13 April 2023 | Accepted: 25 April 2023

DOI: 10.1111/mpp.13352

Molecular Plant Pathology WILEY

ORIGINAL ARTICLE

Verticillium longisporum phospholipase $VlsPLA_2$ is a virulence factor that targets host nuclei and modulates plant immunity

Vahideh Rafiei | Heriberto Vélëz | Edoardo Piombo | Mukesh Dubey | Georgios Tzelepis

Department of Forest Mycology and Plant Pathology, Swedish University of Agricultural Sciences, Uppsala Biocenter, Uppsala, Sweden

Correspondence
Georgios Tzelepis, Department of Forest Mycology and Plant Pathology, Swedish University of Agricultural Sciences, Uppsala Biocenter, Box 7026, SE-750 07 Uppsala, Sweden.
Email: georgios.tzelepis@slu.se

Funding information
Carl Tryggers Stiftelse för Vetenskaplig Forskning, Grant/Award Number: CTS 19:374; Helge Ax:son Johnsons Stiftelse; Svenska Forskningsrådet Formas, Grant/Award Number: 942-2015-36

Abstract

Phospholipase A_2 (PLA_2) is a lipolytic enzyme that hydrolyses phospholipids in the cell membrane. In the present study, we investigated the role of secreted PLA_2 ($VlsPLA_2$) in *Verticillium longisporum*, a fungal phytopathogen that mostly infects plants belonging to the Brassicaceae family, causing severe annual yield loss worldwide. Expression of the *VlsPLA*$_2$ gene, which encodes active PLA_2, is highly induced during the interaction of the fungus with the host plant *Brassica napus*. Heterologous expression of $VlsPLA_2$ in *Nicotiana benthamiana* resulted in increased synthesis of certain phospholipids compared to plants in which enzymatically inactive PLA_2 was expressed ($VlsPLA_2^{\Delta CD}$). Moreover, $VlsPLA_2$ suppresses the hypersensitive response triggered by the Cf4/Avr4 complex, thereby suppressing the chitin-induced reactive oxygen species burst. $VlsPLA_2$-overexpressing *V. longisporum* strains showed increased virulence in *Arabidopsis* plants, and transcriptomic analysis of this fungal strain revealed that the induction of the gene contributed to increased virulence. $VlsPLA_2$ was initially localized to the host nucleus and then translocated to the chloroplasts at later time points. In addition, $VlsPLA_2$ bound to the vesicle-associated membrane protein A (VAMPA) and was transported to the nuclear membrane. In the nucleus, $VlsPLA_2$ caused major alterations in the expression levels of genes encoding transcription factors and subtilisin-like proteases, which play a role in plant immunity. In conclusion, our study showed that $VlsPLA_2$ acts as a virulence factor, possibly by hydrolysing host nuclear envelope phospholipids, which, through a signal transduction cascade, may suppress basal plant immune responses.

KEYWORDS
effector, nucleus, phospholipase, phospholipids, VAMP, *Verticillium*

Vahideh Rafiei and Heriberto Vélëz contributed equally.

1 | INTRODUCTION

Phospholipids are essential structural components of cell membranes and are conserved in living organisms—from bacteria to plants and humans. They form a lipid bilayer with a hydrophobic interior and a hydrophilic exterior; they are abundant in the mitochondrial and nuclear envelopes, whereas they are scarce in thylakoid membranes (Nakamura, 2017). Phospholipases hydrolyse phospholipids to phosphatidic acid, diacylglycerol, free fatty acids, and lysophospholipids. Based on the site of glycerophospholipid hydrolysis, phospholipases are categorized into classes A_1 (PLA_1), A_2 (PLA_2), C (PLC), and D (PLD), which are further subdivided into many families and subfamilies (Aloulou et al., 2012). They play important roles in various aspects of cell physiology, including signal transduction, cytoskeletal dynamics, and protein secretion (Hong et al., 2016). They are also involved in plant defence mechanisms, probably as early signalling molecules (Zhao, 2015). Secreted phospholipases regulate different processes in bacterial and fungal pathogens. However, their precise roles in fungal virulence remain unknown (Ghannoum, 2000; Sitkiewicz et al., 2007).

Plant pathogens produce cell wall-degrading enzymes and a plethora of small proteins, termed effectors, to manipulate plant immune mechanisms and establish successful infection (Giraldo & Valent, 2013; Rafiei et al., 2021). These proteins have diverse functions, including inducing necrosis, suppressing the hypersensitive response (HR), protecting fungal hyphae from host-secreted enzymes, such as chitinases, and manipulating energy production in the host (Lo Presti et al., 2015). The host plant also deploys defence mechanisms to counteract the attack of the pathogen; hence, signalling plays a prominent role in this process. As the first layer, the plasma membrane-localized pattern recognition receptors (PRRs) recognize microbe-associated molecular patterns (e.g., chitin, flagellin), and this recognition can lead to a reactive oxygen species (ROS) burst, influx of calcium (Ca^+), the activation of mitogen-activated protein kinases (MAPKs), and the induction of defence genes, resulting in pattern-triggered immunity (Couto & Zipfel, 2016). Additionally, hosts deploy nucleotide-binding domain leucine-rich repeat-containing proteins (NLRs) that recognize cytoplasmic effectors, leading to effector-triggered immunity (ETI) (Boller & Felix, 2009). The outcome of ETI is typically the induction of HR, although pattern-triggered immunity can also result in programmed cell death (Jones & Dangl, 2006).

The genus *Verticillium*, which belongs to the family Plectosphaerellaceae in the phylum Ascomycota, includes species that cause vascular wilt disease in a plethora of economically important crops. The most important species is the haploid *Verticillium dahliae*, which has a broad host range comprising a large number of dicotyledonous plants (e.g., tomato, cotton, and olive). In contrast, *V. longisporum* has a narrow host range, infecting mostly plants in the Brassicaceae family (e.g., rape seed, cabbage, and broccoli) (Depotter et al., 2016), and it is one of the most prominent pathogens in rape seed (*Brassica napus*) cultivation worldwide (Dunker et al., 2008; Tzelepis et al., 2017). *V. longisporum* is the only nonhaploid species in this genus, and its genome, characterized as amphidiploid, is the result of the hybridization of two species, *V. dahliae* and an unknown species (Inderbitzin et al., 2011).

In this study, we investigated the role of a secreted PLA_2 ($VlsPLA_2$) in the virulence of *V. longisporum*. *$VlsPLA_2$* expression was highly induced during interaction with *B. napus*. We hypothesized that it acts as an effector protein that suppresses the immune response in host plants. Overexpression of this gene in *V. longisporum* resulted in mutants with increased fungal virulence and the up-regulation of genes coding for variable pathogenicity factors. Furthermore, we confirmed that this protein is an active PLA_2 that interacts with vesicle-associated membrane proteins (VAMPs). This interaction possibly facilitates $VlsPLA_2$ transfer to the nuclear envelope and entry into the nucleoplasm, where it alters the expression levels of genes involved in plant defence. Finally, $VlsPLA_2$ suppressed the HR induced by the Cf4/Avr4 complex. Taken together, the results of this study improve the current understanding of the precise roles of these lytic enzymes in fungal infection biology.

2 | RESULTS

2.1 | The *$VlsPLA_2$* gene is highly induced during host infection

V. longisporum isolate VL1 contains more than 80 genes that encode putative candidate effector proteins (Fogelqvist et al., 2018). We prioritized 13 predicted singletons from the VL1 genome and studied their transcription patterns during infection. Among these genes, only seven were expressed during interaction with the host (Figure S1). The *$VlsPLA_2$* gene (*VL1_T00014035*), encoding a putative phospholipase A_2, was highly up-regulated in *V. longisporum* during its interaction with *B. napus* roots compared to mycelia grown in potato dextrose broth (PDB) (Figure S1). The *$VlsPLA_2$* transcription pattern showed the highest induction at 6 days postinfection (dpi) (Figure S1). Because the role of secreted A_2 phospholipases in fungal virulence is not yet fully understood, this gene was selected for further analysis.

2.2 | $VlsPLA_2$ is a functional phospholipase A_2 enzyme

Analysis of the *V. longisporum* genome revealed two alleles of the *$VlsPLA_2$* gene, showing 98% homology (*VL1_T00014035* and *VL1_T00011351*). Conserved domain analysis using translated amino acid sequences of $VlsPLA_2$ identified a conserved phospholipase A_2 domain (IPR015141), which is present in fungal and bacterial phospholipase A_2 enzymes (Matoba et al., 2002), and a signal peptide (SP) at the N-terminus. Furthermore, sequence analysis of $VlsPLA_2$ compared with fungal and bacterial species showed a conserved CxRHDFGYxN motif, including the catalytic dyad (HD) (Figure 1a). Further analysis using multiple prediction tools showed the presence of a chloroplast transit peptide and two nuclear localization signals (NLSs; one monopartite and one bipartite), suggesting that $VlsPLA_2$

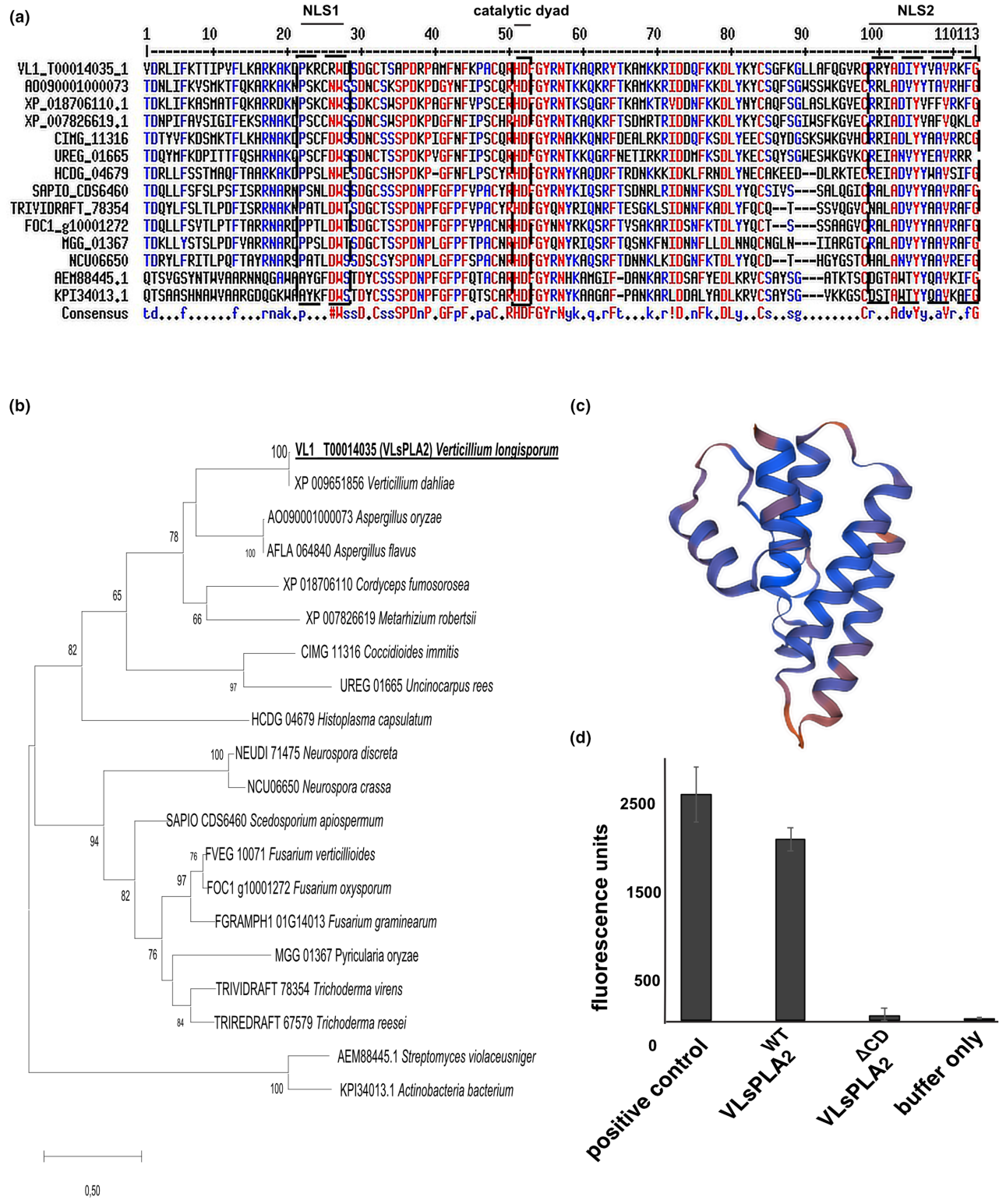

FIGURE 1 Analysis of the VlsPLA$_2$ protein. (a) Alignment of the amino acid sequences of VlsPLA$_2$ and phospholipases derived from different bacterial and fungal species using Clustal Omega software. Identical amino acids are marked with red colour. The catalytic dyad HD and the two nuclear localization signals (NLSs) are marked with dashed boxes. (b) Phylogenetic analysis of the VlsPLA$_2$ protein and phospholipases from different fungal species. Analysis was conducted using the neighbour-joining method with the JTT amino acid substitution model based on amino acid sequences and 1000 bootstraps. Numbers at nodes indicate the bootstrap values. The bar indicates the number of amino acid substitutions. Predicted amino acid sequences were aligned using the ClustalW algorithm and phylogeny was constructed in MEGA X software. (c) Predicted 3D structure of VlsPLA$_2$. The protein model was predicted using SWISS-MODEL software. (d) Phospholipase A$_2$ activity assay using 10 μM purified VlsPLA$_2^{WT}$ and VlsPLA$_2^{\Delta CD}$ proteins. PLA$_2$ from bee venom and buffer only were used as positive and negative controls, respectively. Error bars represent *SE* based on eight technical replicates.

FIGURE 2 The VlsPLA$_2$ phospholipase contributes to *Verticillium longisporum* virulence. (a) *Arabidopsis thaliana* plants infected with *V. longisporum* VlsPLA$_2$+^{WT}, VlsPLA$_2$+$^{\Delta CD}$, or wild-type (WT). The experiment was performed in 36 plants. Photographs of representative plants were taken 28 days postinoculation (dpi). Mock-inoculated plants were used as control. (b) Proportions of dead, mildly infected, and healthy *A. thaliana* plants at 28 dpi with *V. longisporum* VlsPLA$_2$+^{WT}, VlsPLA$_2$+$^{\Delta CD}$, or WT. (c) Rosette size in cm of *A. thaliana* plants infected with *V. longisporum* VlsPLA$_2$+^{WT}, VlsPLA$_2$+$^{\Delta CD}$, or WT at 28 dpi. Different letters (a, b, c) show statistically significant differences according to Student's *t* test ($p < 0.05$). Error bars represent *SE* based on at least 36 plants. (d) Representative *A. thaliana* plants expressing the VlsPLA$_2$ phospholipase (35S::*VlsPLA*$_2$) at 28 dpi with *V. longisporum*. Mock-inoculated and plants expressing free green fluorescent protein (GFP) were used as controls. (e) Percentage of dead, mildly infected, and healthy 35S::*VlsPLA*$_2$, free GFP-expressing, and mock-inoculated *A. thaliana* plants at 28 dpi with *V. longisporum*. (f) Rosette size in cm of 35S::*VlsPLA*$_2$, free GFP-expressing, and mock-inoculated *A. thaliana* plants at 28 dpi with *V. longisporum*. Different letters (a, b, c) show statistically significant differences according to Student's *t* test ($p < 0.05$). Error bars represent *SE* based on at least 50 plants. The background of the images has been removed using Affinity Designer software without disrupting the plant area.

is a putative cytoplasmic effector with nuclear and chloroplast localization (Figure 1a).

To study the gene distribution of *PLA*$_2$ among fungal species, more than 60 genomes from species in the Basidiomycota, Ascomycota, Mucoromycota, and Chytridiomycota divisions were screened. Our analysis showed that genes putatively encoding secreted PLA$_2$ were identified only in Ascomycota species with diverse lifestyles, especially in the classes Sordariomycetes, Dothideomycetes, Eurotiomycetes, and Pezizomycetes (Table S1), with no clear correlation with ecological niches or lifestyles. Phylogenetic analysis of putative PLA$_2$ homologues derived from different fungal species showed that these proteins were grouped into two major clades and that VlsPLA$_2$ clustered together with PLA$_2$ from *V. dahliae*, *Aspergillus* spp., and entomopathogenic genera such as *Metarhizium* and *Cordyceps* (Figure 1b). Analysis of the predicted 3D protein structure revealed 54% identity with PLA$_2$ from the mycorrhizal ascomycete *Tuber borchii* and 48% similarity with PLA$_2$ from the bacterial species *Streptomyces violaceoruber* (Figure 1c).

To investigate phospholipase activity, VlsPLA$_2$ was heterologously expressed in *Escherichia coli* cells. Enzymatic assays with the purified protein showed that VlsPLA$_2$ was an active phospholipase A$_2$ that was able to degrade a PLA$_2$-selective substrate, similar to PLA$_2$ derived from the venom of *Apis mellifera*, which was used as a positive control (Figure 1d). The role of the HD catalytic dyad in the enzymatic activity of VlsPLA$_2$ (Murakami & Kudo, 2004) was investigated by replacing both amino acids with alanine. Our results showed that the mutated isoform of VlsPLA$_2$ (i.e., VlsPLA$_2^{\Delta CD}$) was not able to degrade the selective substrate, indicating that this dyad is important for its enzymatic function (Figure 1d).

2.3 | Heterologous expression of VlsPLA$_2$ in *Nicotiana benthamiana* alters the phospholipid profile in the plant

Because phospholipases influence the phospholipid composition within cells, a lipidomic analysis was conducted to investigate whether VlsPLA$_2$ was able to alter the phospholipid profile in plants. Thus, the wild-type (WT) and the catalytically inactive isoform of this protein (i.e., VlsPLA$_2^{\Delta CD}$) were heterologously expressed in *N. benthamiana* and the lipid profiles of the plants were analysed. We focused our analysis mostly on phospholipid classes that are abundant in plant cell membranes, such as phosphatidylcholine and phosphatidylethanolamine (Nakamura, 2017). Our data showed that the relative amounts of monoacyl-glycero-phosphocholines 16:0 and diacyl-glycero-phosphocholines 36:5 and 36:6 were significantly increased in plants expressing VlsPLA$_2^{WT}$ compared to the VlsPLA$_2^{\Delta CD}$ or mock-inoculated ones (Figure S2), indicating that this phospholipase has an impact on the host's phospholipid profile.

2.4 | *VlsPLA*$_2$ contributes to the virulence of *V. longisporum*

To evaluate the potential involvement of VlsPLA$_2$ in *V. longisporum* virulence, a deletion strain was constructed. Interestingly, all efforts to delete this gene, either in *V. longisporum* or *V. dahliae*, resulted in mutants carrying both the deleted locus and the WT gene (data not shown). Attempts to segregate the mutated nucleus via multiple single-spore isolations failed continuously. Therefore, mutants overexpressing the *VlsPLA*$_2$ gene in *V. longisporum* were generated. The transcription analysis of six single-spore isolates, three overexpressing the WT (i.e., *VlsPLA*$_2$+^{WT}) and three overexpressing the enzymatically inactive gene (i.e., *VlsPLA*$_2$+$^{\Delta CD}$), showed a significant increase of *VlsPLA*$_2$ transcription levels in comparison to WT (Figure S3). Isolates *VlsPLA*$_2$+^{WT} (3) and *VlsPLA*$_2$+$^{\Delta CD}$ (1) were chosen for further analysis because they showed similar expression levels (Figure S3).

Arabidopsis thaliana plants were inoculated with the *V. longisporum* WT or overexpression strains, and plant growth and disease symptoms were monitored at 28 dpi. We observed that plants infected with the *VlsPLA*$_2$+^{WT} strain showed more severe symptoms and smaller rosettes compared to plants infected with the WT and *VlsPLA*$_2$+$^{\Delta CD}$ strains. A higher number of dead plants were observed upon infection with the *VlsPLA*$_2$+^{WT} strain compared to the *VlsPLA*$_2$+$^{\Delta CD}$ one (Figure 2a–c).

The role of this phospholipase in virulence was investigated by generating *A. thaliana* lines expressing the *VlsPLA*$_2$ gene. Our results showed that the expression lines (35S::*VlsPLA*$_2$) displayed a higher percentage of dead plants and smaller rosettes than infected plants expressing only free green fluorescent protein (GFP), indicating that VlsPLA$_2$ contributes to *V. longisporum* virulence (Figure 2d–f).

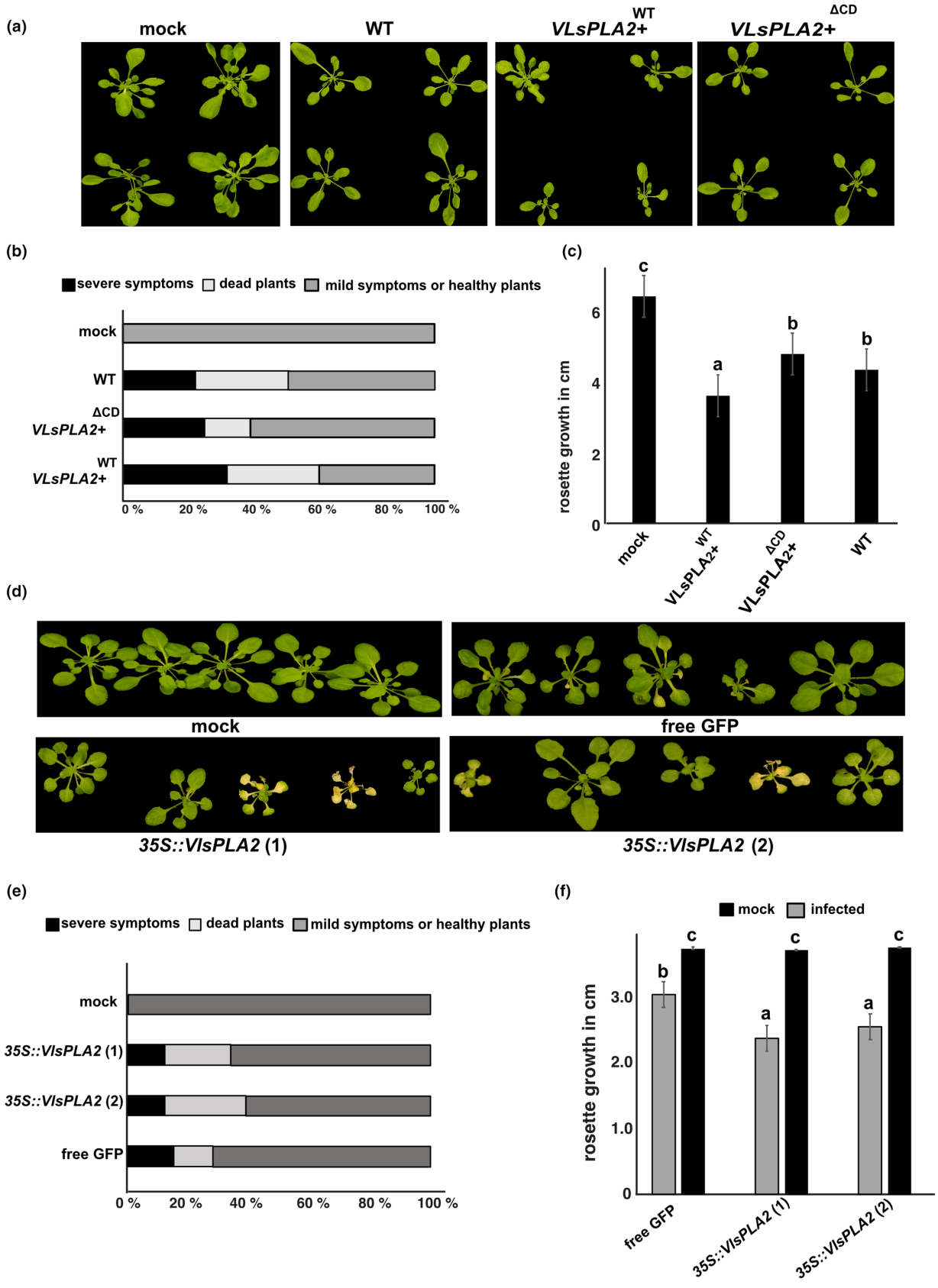

Because $VlsPLA_2$ was highly expressed in *V. longisporum* during interaction with *B. napus* (Figure S1), we analysed the transcriptome of the $VlsPLA_2$+^{WT} strain to investigate the potential transcriptomic changes through which up-regulation of this gene could enhance the growth of *V. longisporum* mycelia during infection. Our data showed that more than 1300 genes were differentially regulated in the $VlsPLA_2$+^{WT} strain compared with the WT strain (Figure 3a; Table S2). To test whether these transcriptional changes in the

VlsPLA$_2$+^{WT} strain were associated with its enhanced phospholipase activity, the transcriptome of the *VlsPLA*$_2$+$^{\Delta CD}$ strain was also analysed. In contrast to the *VlsPLA*$_2$+^{WT} strain, only 104 genes were differentially expressed in the *VlsPLA*$_2$+$^{\Delta CD}$ strain compared to the WT (Figure 3a; Table S2). Moreover, among these 1300 genes, 158 were up-regulated in the *VlsPLA*$_2$$^{+WT}$ strain compared to both *VlsPLA*$_2$+$^{\Delta CD}$ and WT (Figure 3a). Among them, we identified several genes that have been validated for their role in *Verticillium* virulence (Santhanam & Thomma, 2013; Tian et al., 2017; Zhang et al., 2016), such as genes encoding zinc finger proteins, cytochrome monooxygenases, efflux pump proteins, and a calpain-A-like protein (Figure 3b; Table S3), indicating that *VlsPLA*$_2$ influences the expression levels of pathogenicity-related genes in *V. longisporum*.

2.5 | VlsPLA$_2$ suppresses HR induced by the Avr4/Cf4 complex

Pathogens, particularly necrotrophs, secrete numerous necrosis-inducing effectors (Lo Presti et al., 2015). Therefore, we investigated whether VlsPLA$_2$ could have the same function by transiently expressing VlsPLA$_2$ in *N. benthamiana* plants and monitoring the symptoms daily. No necrosis was observed even 7 days after agroinfiltration (data not shown). Moreover, many pathogens rely on the initial biotrophic stage to establish a successful infection by secreting HR-suppressing effectors (Lo Presti et al., 2015). Hence, the ability of VlsPLA$_2$ to suppress a PRR-mediated HR, induced by the Cf4/Avr4 complex was investigated (Joosten et al., 1997). Our results showed that in the area where VlsPLA$_2$^{WT} was previously agroinfiltrated, a significant reduction in HR was observed compared to the areas where mock inoculation was applied or the empty vector control was infiltrated (Figure 4a). In contrast, the enzymatically inactive isoform (VlsPLA$_2$$^{\Delta CD}$) was unable to suppress the HR (Figure 4a). Furthermore, the role of VlsPLA$_2$ in suppressing HR was investigated using the bacterial strain *Pseudomonas syringae* pv. *tomato* DC3000, which secretes effectors into the host through a type III secretion system recognized by *N. benthamiana* resistance proteins, leading to a strong HR (Collmer et al., 2002). Our results showed that VlsPLA$_2$ was unable to suppress HR in this complex, indicating that this effector is mainly involved in the suppression of basal immune responses (Figure 4b).

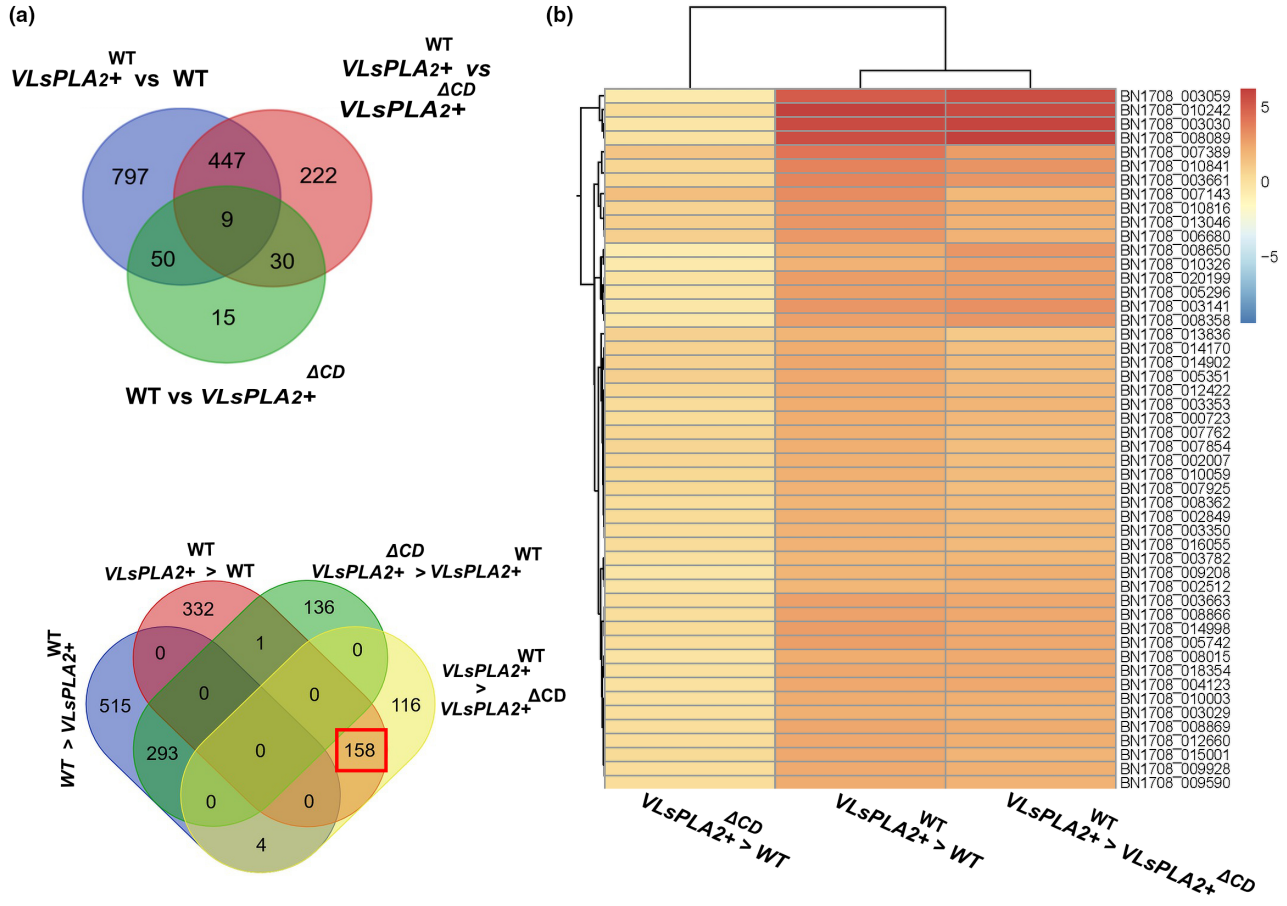

FIGURE 3 Overexpression of *VlsPLA*$_2$ causes major transcriptomic changes in *Verticillium longisporum* mycelia. (a) Venn diagrams showing the numbers of differentially expressed genes in *V. longisporum* mycelia derived from the wild type (WT) and strains overexpressing either the functionally active (VlsPLA$_2$+^{WT}) or the inactive (VlsPLA$_2$+$^{\Delta CD}$) VlsPLA$_2$ phospholipase. The sign ">" shows the number of up-regulated genes in each comparison. The number of genes of interest is highlighted in a red box. (b) Heatmap depicting the top 50 up-regulated genes in the *V. longisporum* VlsPLA$_2$+^{WT} strain as compared to VlsPLA$_2$+$^{\Delta CD}$ and WT. Adjusted p-value <0.05 and $\log_2$(fold change) >1 for up-regulated genes. Analysis involved four biological replicates.

To investigate whether VlsPLA$_2$ could suppress the ROS burst, a luminol-based assay was performed on *N. benthamiana* leaves. The ROS burst was significantly induced by chitin, and ROS production was significantly reduced in leaves that had previously been treated with the VlsPLA$_2^{WT}$ protein compared to nontreated leaves (Figure 4c). In contrast, no ROS suppression was observed in leaves treated with the enzymatically inactive protein (i.e., VlsPLA$_2^{\Delta CD}$), suggesting that suppression of HR was possibly attributed to the suppression of ROS burst (Figure 4c).

2.6 | VlsPLA$_2$ is initially localized to the host nuclei

As mentioned previously, the VlsPLA$_2$ protein sequence contains two putative NLS motifs (Figure 1a). Thus, to confirm the predicted subcellular localization of VlsPLA$_2$, a construct was generated by tagging VlsPLA$_2$ with GFP at the C-terminus, keeping its SP intact, and transiently expressed in *N. benthamiana* leaves, which were monitored using a confocal microscope at 48 and 72 h postinfiltration (hpi). Our observations showed that the protein was clearly localized to the host nuclei at 48 hpi, whereas it was translocated to chloroplasts and the cell periphery at 72 hpi (Figure 5a). To investigate whether the predicted NLSs were functional, a truncated isoform of VlsPLA$_2$ was constructed where both NLSs were disrupted (i.e., VlsPLA$_2^{\Delta NLS1NLS2}$). Confocal microscopy revealed that this truncated isoform was localized at the cell periphery, but no nuclear localization was observed (Figure 5b). Furthermore, we investigated whether both NLSs are critical for nuclear localization. Therefore, truncated isoforms were constructed where either NLS1 or NLS2 was deleted (i.e., VlsPLA$_2^{\Delta NLS1}$ and VlsPLA$_2^{\Delta NLS2}$). Our analysis showed that while both NLS mutants were functional, the bipartite NLS2 was more important for nuclear localization (Figure S4). We also studied whether deletion of its native SP could affect VlsPLA$_2$ localization. Therefore, an isoform lacking this signal was constructed (i.e., VlsPLA$_2^{\Delta SP}$). No changes in subcellular localization were observed between the WT and VlsPLA$_2^{\Delta SP}$ isoforms (Figure S4). We also investigated the localization of the VlsPLA$_2^{\Delta CD}$ isoform at 48 hpi. Interestingly, we observed that VlsPLA$_2^{\Delta CD}$ was localized in the chloroplasts and was unable to enter the nucleus, although both NLSs were intact, indicating that additional factors could also be involved in its nuclear localization (Figure 5c).

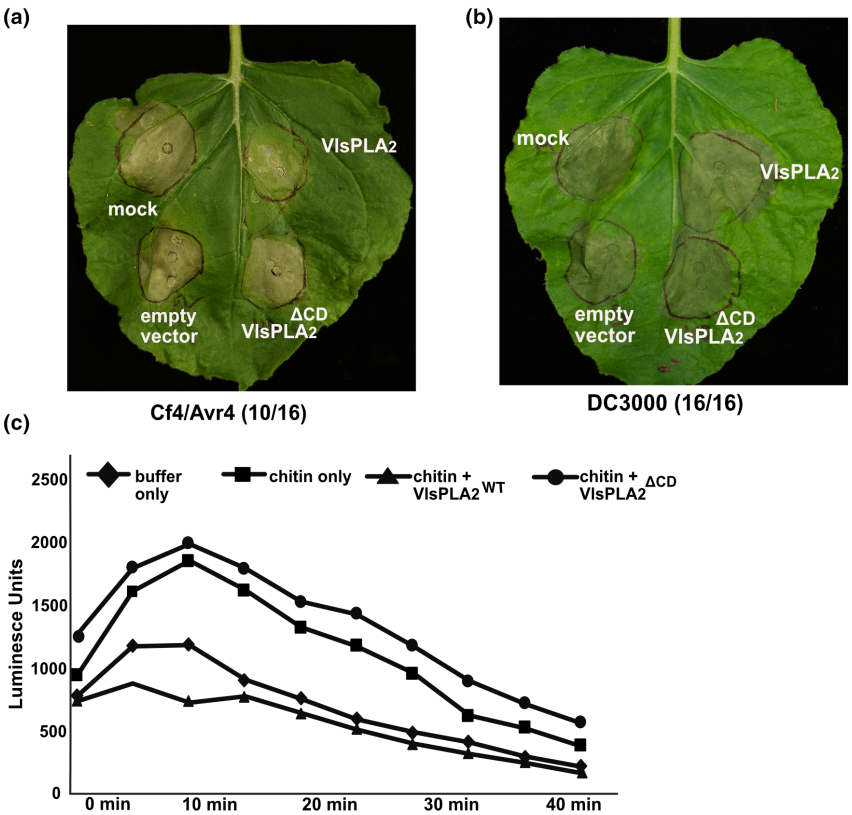

FIGURE 4 The VlsPLA$_2$ phospholipase negatively regulates the hypersensitive response (HR) induced by the Avr4/Cf4 complex. (a) HR suppression assay by VlsPLA$_2^{WT}$ and VlsPLA$_2^{\Delta CD}$ on *Nicotiana benthamiana* expressing the Cf4 receptor. HR was detected 24 h postinfiltration (hpi) with the Avr4 effector. (b) HR suppression assay using VlsPLA$_2^{WT}$ and VlsPLA$_2^{\Delta CD}$ on *N. benthamiana*. HR was induced by *Pseudomonas syringae* pv. *tomato* DC3000 at 24 hpi. Inoculation with the empty pGWB602 vector and mock inoculation with induction buffer were used as controls. Images were collected 3 days postinoculation. In total, eight plants (two leaves per plant) were used. (c) Chitin-induced reactive oxygen species (ROS) burst assay in *N. benthamiana* leaves. Production of ROS was determined using luminol-dependent chemiluminescence. Leaf discs were treated with chitin, 10 μM purified VlsPLA$_2^{WT}$ protein, or 10 μM purified VlsPLA$_2^{\Delta CD}$ protein, while only buffer was used as a negative control. In total, eight biological replicates were used.

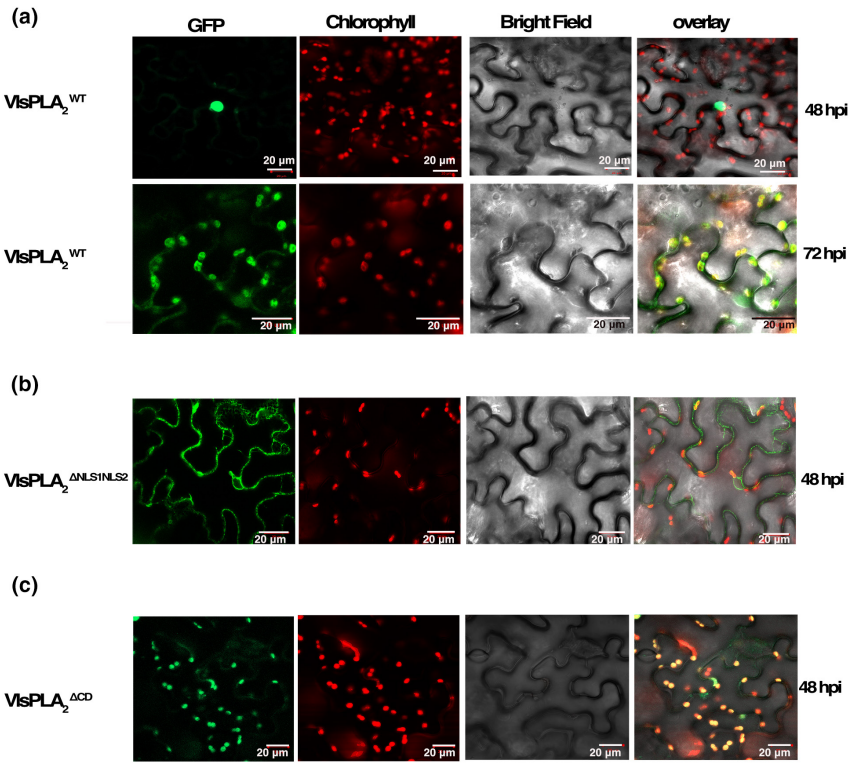

FIGURE 5 The VlsPLA$_2$ phospholipase is initially localized to the host nuclei. Live cell imaging of (a) VlsPLA$_2^{WT}$, (b) VlsPLA$_2^{\Delta NLS1NLS2}$, and (c) VlsPLA$_2^{\Delta CD}$ tagged with green fluorescent protein (GFP) at the C-terminus after transient expression in *Nicotiana benthamiana* leaves. The localization was monitored with a laser-scanning confocal microscope in sequential scanning mode at 48 and 72 h postinfiltration. GFP and chlorophyll were excited at 488 nm. GFP (green) and chlorophyll (red) fluorescence signals were detected at 505–525 and 680–700 nm, respectively.

2.7 | VlsPLA$_2$ binds to vesicle-associated membrane protein A

To investigate whether VlsPLA$_2$ interacts with plant proteins, VlsPLA$_2$::GFP-CT was transiently expressed in *N. benthamiana*, pulled down at 48 hpi using GFP-trapped beads, and processed for tandem mass spectrometry (MS/MS). In our analysis, a plethora of potential interactions were identified compared to the free GFP control (Table S4). As MS/MS analysis showed that VlsPLA$_2$ potentially interacts with various membrane vesicle proteins, their interactions were further investigated using yeast two-hybrid (Y2H) assays (Table S4). Our results showed that the yeast strains co-transformed with VlsPLA$_2$ and NbS00011956g0004, which is a putative vesicle-associated membrane protein A (VAMPA), denoted as NbVAMPA1, were able to grow on auxotrophic selection plates (−His, −Ade, −Leu, −Trp), suggesting potential interactions between them (Figure 6a). Furthermore, disruption of the NLSs did not have any appreciable impact on this interaction (Figure 6a). However, co-immunoprecipitation (co-IP) assays showed that NbVAMPA1 interacted only with the VlsPLA$_2^{\Delta NLS1NLS2}$ isoform (Figure 6b). This may be attributed to the localization and amount of the VlsPLA$_2^{\Delta NLS1NLS2}$ protein compared to the WT. Confocal microscopy confirmed that NbVAMPA1 was localized to the cell periphery and colocalized with VlsPLA$_2$ in the plant nuclear membrane (Figures 6c and S5a). In addition, we investigated whether VlsPLA$_2^{\Delta CD}$ was able to interact with NbVAMPA1; interestingly, our results showed no interaction between them (Figure 6a). Furthermore, prediction of the VlsPLA$_2^{\Delta CD}$ 3D structure showed that this mutation did not cause any major changes in the protein structure, suggesting that the catalytic dyad HD was responsible for the interaction with this vesicle protein.

NbVAMPA1 protein structure analysis revealed the presence of a motile sperm protein (MSP) domain, an ER-anchored receptor domain involved in interorganelle contacts (Di Mattia et al., 2018), at the N-terminus and a transmembrane domain at the C-terminus. Furthermore, genome analysis of *N. benthamiana* revealed the presence of 10 genes that are homologues of *NbVAMPA1*. Alignment of these 10 homologues revealed the presence of a conserved motif of nine amino acids (DMQCKDKFL) (Figure S5b). Therefore, the roles of different domains (MSP and the transmembrane domain) were analysed using mutants (i.e., NbVAMPA1$^{\Delta MSP}$ and NbVAMPA1$^{\Delta TM}$, respectively). Our results showed that the mutant with the MSP domain only (NbVAMPA1$^{\Delta TM}$) was not able to interact with VlsPLA$_2$, similar to the truncated NbVAMPA1 where the MSP domain had been deleted (NbVAMPA1$^{\Delta MSP}$), indicating that the intact vesicle protein is required for interaction with the VlsPLA$_2$ phospholipase (Figure S5c). Moreover, the importance of the conserved DMQCKDKFL motif in interactions with VlsPLA$_2$ was investigated. Therefore, this conserved motif was deleted (NbVAMPA1$^{\Delta CM}$) and protein interactions were evaluated. Our results showed no interaction between VlsPLA$_2$ and the NbVAMPA1$^{\Delta CM}$ isoform, suggesting that this conserved motif is also important for binding to VlsPLA$_2$ (Figure S5c).

2.8 | *VlsPLA$_2$* modulates expression levels of transcription factors and genes involved in plant immunity

To investigate whether the presence of VlsPLA$_2$ could cause any modification in the plant's gene expression patterns, the transcriptome of *N. benthamiana* leaves that transiently expressed

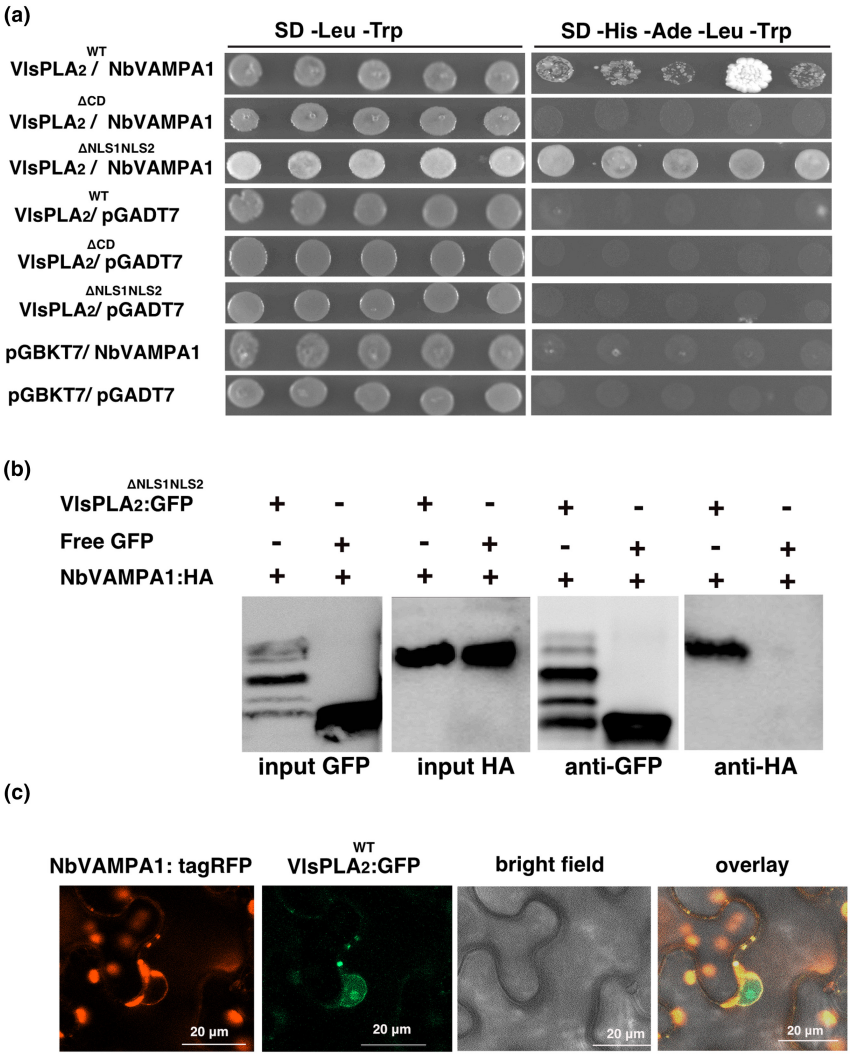

FIGURE 6 The VlsPLA$_2$ phospholipase interacts with the plant vesicle protein NbVAMPA1. (a) Pairwise yeast two-hybrid assays between VlsPLA$_2^{WT}$, VlsPLA$_2^{\Delta CD}$, or VlsPLA$_2^{\Delta NLS1NLS2}$ (used as a bait in the pGBKT7 vector) and NbVAMPA1 (used as a prey in the pGADT7 vector). Growth of yeast cells on SD−4 (−His, −Ade, −Leu, −Trp) selective medium represents protein–protein interaction, and growth on SD−2 (−Leu, −Trp) medium confirms yeast transformation. Yeast transformed with the empty vectors were used as negative controls. (b) Coimmunoprecipitation (co-IP) assay between the GFP-tagged VlsPLA$_2^{\Delta NLS1NLS2}$ and HA-tagged NbVAMPA1 transiently co-expressed in *Nicotiana benthamiana* leaves and pulled down using GFP-trap agarose magnetic beads. (c) Live cell imaging of VlsPLA$_2^{WT}$ tagged with GFP at the C-terminus and NbVAMPA1 tagged with tagRFP at the N-terminus in agroinfiltrated *N. benthamiana* leaves. The localization was monitored with a laser-scanning confocal microscope in sequential scanning mode at 48 h postinfiltration. GFP and chlorophyll were excited at 488 nm. GFP (green) and chlorophyll (red) fluorescence signals were detected at 505–525 and 680–700 nm, respectively. tagRFP was excited at 558 nm and emission was detected at 545–620 nm.

VlsPLA$_2^{WT}$ or *VlsPLA*$_2^{\Delta CD}$ was analysed at 48 and 72 hpi. *N. benthamiana* leaves transiently expressing the empty vector were used as controls. At 48 hpi, 1846 genes were differentially expressed (DEGs) in leaves where the *VlsPLA*$_2^{WT}$ gene was expressed, as compared to 144 genes in plants expressing *VlsPLA*$_2^{\Delta CD}$ (Figure 7a, Table S5). Among these DEGs, 788 were up-regulated and 1062 were down-regulated (Figure 7a; Table S5). Interestingly, the number of DEGs was significantly reduced to 168 at 72 hpi; 127 were induced, and 52 were suppressed (Figure 7a; Table S5).

As VlsPLA$_2$ initially targets the plant nucleus, we investigated the transcription patterns of genes that putatively encode transcription factors. At 48 hpi, in plants where *VlsPLA*$_2^{WT}$ was expressed, we found 22 DEGs encoding transcription factors compared to plants expressing *VlsPLA*$_2^{\Delta CD}$ or the empty vector (Figure 7b; Table S5). Among them, three were induced and 19 were suppressed (Figure 7b; Table S5). Among the down-regulated genes, we identified four encoding ethylene-responsive transcription factors, four encoding basic helix–loop–helix (bHLH) transcription factors, and five encoding myeloblastosis (MYB) transcription factors (Figure 7b; Table S5). Moreover, we investigated whether VlsPLA$_2$ could modulate the expression of genes involved in plant immunity. At 48 hpi, our data showed that six genes encoding putative receptor-like protein kinases (RLKs) and five genes encoding Avr9/Cf-9 rapidly elicited proteins (ACRE) were highly induced in plants expressing

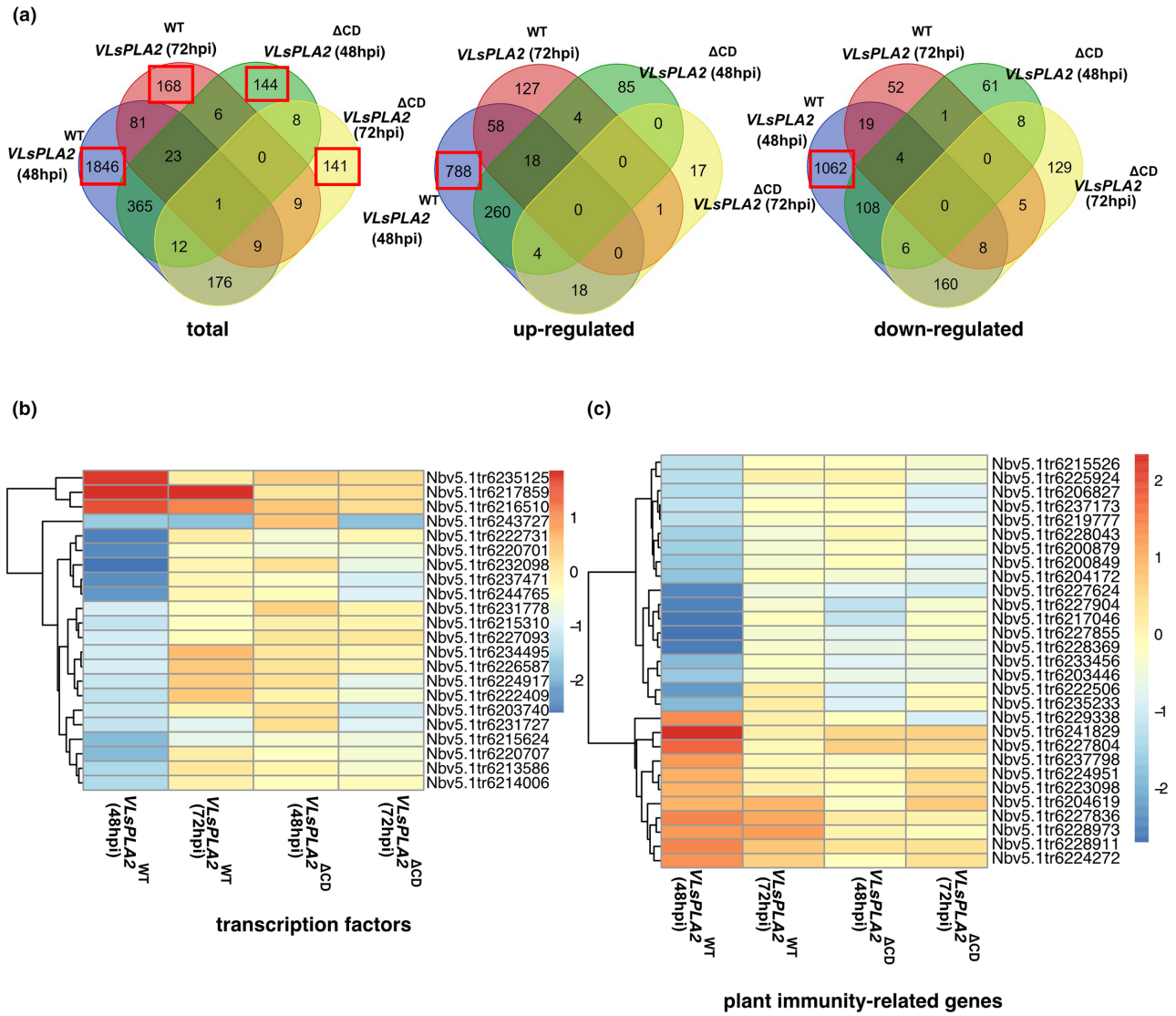

FIGURE 7 The VlsPLA$_2$ phospholipase modulates plant immunity responses. (a) Venn diagrams showing the numbers of differentially expressed genes in *Nicotiana benthamiana* plants transiently expressing either the functionally active (VlsPLA$_2^{WT}$) or the inactive (VlsPLA$_2^{\Delta CD}$) VlsPLA$_2$ phospholipase at 48 and 72 h postinfiltration (hpi). The numbers of genes of interest are highlighted in red boxes. (b) Heatmap depicting the differentially regulated genes putatively encoding transcription factors in *N. benthamiana* plants transiently expressing either VlsPLA$_2^{WT}$ or VlsPLA$_2^{\Delta CD}$ at 48 and 72 hpi. (c) Heatmap depicting the differentially regulated genes putatively encoding plant immunity-related proteins in *N. benthamiana* transiently expressing either VlsPLA$_2^{WT}$ or VlsPLA$_2^{\Delta CD}$ at 48 and 72 hpi. Data were normalized using the transcriptome of empty vector-infiltrated plants (adjusted p-value <0.05, $\log_2$(fold change) >1 for up-regulated genes, and $\log_2$(fold change) <-1 for down-regulated genes). Analysis involved four biological replicates.

VlsPLA$_2^{WT}$ compared to plants with *VlsPLA*$_2^{\Delta CD}$ or the empty vector (Figure 7c; Table S5). In contrast, *VlsPLA*$_2^{WT}$ expression led to the suppression of 14 genes encoding putative subtilisin-like proteases and F-box proteins and three genes encoding aquaporins (Figure 7c; Table S5). In summary, these data indicate that VlsPLA$_2$ is a strong modulator of plant immune responses.

3 | DISCUSSION

In the current study, we investigated the functional role of a fungal-secreted PLA$_2$ enzyme, with emphasis on its involvement in the infection biology of the phytopathogen *V. longisporum*. Previous studies on the role of secreted PLA$_2$ in virulence have been conducted mainly in bacterial–mammalian cell interactions, in which they have been shown to function as toxins that induce proteolysis and haemolysis (e.g., ExoU produced by *Pseudomonas aeruginosa* and SlaA produced by Group A *Streptococcus*), thereby increasing disease severity (Beres et al., 2002; Berthelot et al., 2003). It has been proposed that secreted bacterial PLA$_2$ can degrade phospholipid components in host cell membranes, releasing arachidonic acid, followed by the synthesis of eicosanoids, which interfere with signal transduction cascades, alter the transcription of genes, and lead to increased inflammatory responses (Sitkiewicz

et al., 2007). A similar function could be speculated for the VlsPLA$_2$ phospholipase during its interactions with the plant host. Our data showed that overexpression of *VlsPLA*$_2$ in fungal cells resulted in increased *V. longisporum* virulence, and heterologous expression of this phospholipase in *A. thaliana* led to increased susceptibility to this pathogen. To establish a mechanistic connection between *VlsPLA*$_2$ overexpression and increased virulence, the transcriptomes of *V. longisporum* mycelia and *N. benthamiana* expressing *VlsPLA*$_2$ were analysed. Induced expression of a diverse range of virulence factor genes has been observed (Santhanam & Thomma, 2013; Tian et al., 2017; Zhang et al., 2016), indicating that this phospholipase is involved in signal transduction cascades in fungal cells, altering gene expression levels and leading to increased virulence. Similarly, transcriptomic analysis of *N. benthamiana* leaves showed that VlsPLA$_2$ induces expression of RLKs and ACREs, which are proteins involved in signalling pathways controlling the initial stages of defence responses (Rowland et al., 2005). We also observed that this phospholipase suppressed many genes encoding MYB and bHLH transcription factors in plants. These types of transcription factors have been shown to be involved in the regulation of plant defence mechanisms, such as jasmonic acid-mediated and HR-triggered responses (Pireyre & Burow, 2015). In addition, expression of VlsPLA$_2$ led to the suppression of several genes encoding subtilisin-like proteases and F-box proteins. Their role in the activation of downstream immune responses, including their involvement in the HR, has been demonstrated (Charova et al., 2020; Figueiredo et al., 2014; van den Burg et al., 2008). Moreover, these data were supported by the finding that VlsPLA$_2$ suppressed cell surface PRR-induced HR, but not HR induced by intracellular immune receptors. We hypothesize that VlsPLA$_2$ can only affect membrane-localized immune receptors because of its hydrolysing effect on membranes, whereas cytoplasmic receptors remain unaffected, indicating that this phospholipase is involved mainly in the suppression of basal immune responses.

Nuclear localization of PLA$_2$ has previously been observed in human endothelial cells and *A. thaliana* plants (Froidure et al., 2010; Grewal et al., 2002). In *A. thaliana*, PLA$_2$ suppresses cell death, similarly to VlsPLA$_2$ (Froidure et al., 2010). It has previously been shown that nuclear translocation of cytosolic PLA$_2$ elicits localized hydrolysis of phospholipids in rat cells (Peters-Golden et al., 1996). This agrees with our data showing that VlsPLA$_2$ increases the production of certain phospholipids, suggesting that the products of this enzymatic function are possibly involved in signal transduction pathways and alter the expression levels of genes involved in plant immunity. We also found that the VlsPLA$_2$ phospholipase was associated with plant VAMPA. These are highly conserved proteins present in all eukaryotes and are involved in several physiological processes, including membrane trafficking, lipid transport, and the unfolded protein response (Lev et al., 2008). It has been shown that VAMPs could interact with many different proteins, including proteins involved in plant resistance against fungal pathogens (Kim et al., 2014; Petersen et al., 2009; Saravanan et al., 2009). Our data showed that NbVAMPA1 promotes the entry of VlsPLA$_2$ into the plant nucleoplasmic reticulum, presumably by binding to the active site of VlsPLA$_2$. Similar results have been observed in mammalian cells, where VAMPA and oxysterol-binding proteins promote the entry of endosomes into the nuclear envelope (Santos et al., 2018).

In conclusion, the role of a secreted VlsPLA$_2$ enzyme in the virulence of the phytopathogenic fungus *V. longisporum* was investigated. This phospholipase regulates fungal genes involved in virulence and targets plant nuclei by hijacking VAMP membrane proteins. VlsPLA$_2$ suppresses the expression of genes that play crucial roles in the induction of basal immune responses, possibly through phospholipid production and their involvement in signal transduction cascades. To the best of our knowledge, this study is the first to examine in detail a fungal-secreted PLA$_2$, providing important insight into its role in fungal infection biology.

4 | EXPERIMENTAL PROCEDURES

4.1 | Fungal strains and nucleic acid manipulation

In the current study, *V. longisporum* isolate VL1 (CBS110220) was used. DNA was extracted using a NucleoSpin Plant II kit (Macherey-Nagel GmbH), and RNA was extracted using a Spectrum Plant Total RNA kit (Sigma). RNA was reverse transcribed using the iScript cDNA synthesis kit (Bio-Rad), and quantitative PCR (qPCR) analysis was performed using SsoFast EvaGreen Supermix (Bio-Rad). All PCRs were performed using Phusion Hot Start II High-Fidelity PCR Master Mix (Thermo Scientific).

4.2 | Gene expression analysis

The transcriptional profiles of *V. longisporum* genes encoding candidate effector proteins were investigated as previously described (Rafiei, Najafi, et al., 2022). Briefly, *B. napus* 'Hannah' seedlings were inoculated with *V. longisporum* and harvested at 2, 4, 6, 8, and 10 dpi, while mycelia grown in PDB (Difco) were used as a control. RNA was extracted and treated with DNase I (Thermo Fisher Scientific). For reverse transcription (RT)-qPCR, 1 μg of total RNA was reverse transcribed and used for the analysis. Primer sequences are listed in Table S6. Gene expression levels were normalized to that of the reference gene glyceraldehyde phosphate dehydrogenase (*GAPDH*) (Rafiei, Ruffino, et al., 2022). Relative expression values were calculated from the threshold cycle (C_t) values according to the $2^{-\Delta\Delta Ct}$ method (Livak & Schmittgen, 2001).

4.3 | Protein sequence analysis, structure prediction, and phylogeny

The amino acid sequence of VlsPLA$_2$ was retrieved from the *V. longisporum* VL1 genome (Fogelqvist et al., 2018). Conserved domains were analysed using the SMART protein tools (Letunic

et al., 2009). To investigate whether VlsPLA$_2$ is an apoplastic or cytoplasmic effector, the ApoplastP prediction tool was used, and its subcellular localization was predicted using LOCALIZER software (Sperschneider et al., 2017, 2018). For the phylogenetic analysis, amino acid sequences of homologues of VlsPLA$_2$ were aligned using ClustalW and analysed in MEGA X using the JTT amino acid substitution model, and the VlsPLA$_2$ 3D structure was predicted using the SWISS-MODEL server (Kumar et al., 2018; Waterhouse et al., 2018).

4.4 | Plasmids and vectors

Gene fragments for VlsPLA$_2$ and NbVAMPA1 WT and truncated isoforms were amplified from *V. longisporum* and *N. benthamiana* cDNA, respectively, or synthesized by Integrated DNA Technologies. The vectors used in the present study are listed in Table S7. To overexpress VlsPLA$_2$+^{WT} or VlsPLA$_2$+$^{\Delta CD}$ in the fungus, a pRFHUE vector was used, which contains the constitutively expressed *gpdA* promoter (Crespo-Sempere et al., 2011).

4.5 | Heterologous protein expression and enzymatic activity assay

Subcloning, expression, and purification of active (VlsPLA$_2^{WT}$) and inactive (VlsPLA$_2^{\Delta CD}$) proteins were performed using the Protein Expertise Platform at Umeå University. Briefly, *E. coli* Origami2 (DE3) cells were used and protein expression was induced by the addition of 0.4 mM isopropyl β-D-1-thiogalactopyranoside. The target protein was purified using His-tag purification resin (Roche) according to the manufacturer's instructions. For the phospholipase A$_2$ enzymatic activity assay, the EnzChek Phospholipase A$_2$ Activity Kit was used (Thermo Fisher Scientific) according to the manufacturer's instructions. In all assays, 10 μM of pure active (VlsPLA$_2^{WT}$) or inactive (VlsPLA$_2^{\Delta CD}$) protein was used.

4.6 | Lipidomic analysis

For the lipidomic analysis, overnight cultures of *Agrobacterium tumefaciens* C58C1 harbouring pGWB602-VlsPLA$_2^{WT}$, pGWB602-VlsPLA$_2^{\Delta CD}$, or the empty vector (i.e., pGWB602) were infiltrated in leaves of 4-week-old *N. benthamiana* plants (grown under an 18 h light/6 h dark photoperiod at 23°C). Leaves were harvested at 48 hpi and lipids were extracted using a chloroform:methanol (2:1) phase extraction method. The chloroform phase was used for UHPLC-QTOF-MS/MS analysis using a 1290 Infinity UHPLC (Agilent) coupled to a QTOF 6546 instrument (ODIN) (Agilent) using the parameters previously described for this type of analysis (Nygren et al., 2011). Data analysis was conducted using ProFinder software (v. 10.0; Agilent Technologies) by comparing the peaks with internal database standards for different lipid classes.

4.7 | Fungal transformation and virulence assays

The vectors pRFHUE-VlsPLA$_2^{WT}$ and pRFHUE-VlsPLA$_2^{\Delta CD}$ were transformed into *V. longisporum* using an *Agrobacterium*-based protocol (Utermark & Karlovsky, 2008). The expression levels of the *VlsPLA$_2$* gene in the mutant strains were investigated by RT-qPCR as described above. Single-spore cultures were prepared using the five colonies with the highest expression and used for virulence assays. *A. thaliana* was used for virulence assays. Plants were infected with *V. longisporum* WT and overexpression strains (i.e., *VlsPLA$_2^{WT}$* and *VlsPLA$_2^{\Delta CD}$*) or mock-inoculated as described above for the transcription analysis and grown in short-day conditions (8 h light/16 h dark) at 23°C/18°C for 4 weeks. Disease severity was categorized as healthy, mildly infected, severely infected, or dead. In addition, rosette diameter was measured at 28 dpi.

4.8 | Construction of transgenic *A. thaliana* plants

A. tumefaciens C58C1 cells carrying the vector pGWB605-VlsPLA$_2^{WT}$ were used to transform *A. thaliana* Col-0 using the floral dip method with 50 μg/mL of BASTA (glufosinate ammonium) to select for transformants. The expression levels of VlsPLA$_2^{WT}$ in the transgenic lines were confirmed using RT-PCR and western blotting. Two independent homogenous lines in the T$_4$ generation were used for virulence assays as described above.

4.9 | Live cell imaging, HR suppression assay, and ROS burst suppression assay

Overnight cultures of *A. tumefaciens* C58C1 harbouring the vectors shown in Table S7 were infiltrated on leaves of 4-week-old *N. benthamiana* plants (grown under an 18 h light/6 h dark photoperiod at 23°C), The subcellular localization of the phospholipase was monitored using a confocal microscope (LSM 800; Zeiss) at 48 and 72 hpi.

For the HR suppression assay, the pGWB602-VlsPLA$_2^{WT}$ and pGWB602-VlsPLA$_2^{\Delta CD}$ vectors were transiently expressed in *N. benthamiana* plants harbouring the Cf4 receptor protein from tomato plants as previously described (Charova et al., 2020). The ability of VlsPLA$_2$ to suppress ETI-triggered HR was investigated on *N. benthamiana* WT plants infected with *P. syringae* pv. *tomato* DC3000. Agroinfiltration with an empty vector and induction buffer alone (mock) were used as controls. For the ROS burst suppression assay, a luminol-based protocol was used. Briefly, leaf discs from *N. benthamiana* plants were treated with chitin (100 μL/mL), luminol (200 μM) (Sigma), and 10 μg/mL horseradish peroxidase (Sigma). The suppression of ROS burst was analysed by using 10 μM VlsPLA$_2^{WT}$ and VlsPLA$_2^{\Delta CD}$ proteins and measuring the chemiluminescence signals using a BMG LABTECH microplate reader.

4.10 | MS/MS assay

The pGWB605-VlsPLA$_2^{WT}$ vector was transiently expressed in *N. benthamiana*, and the free GFP vector was used as a negative control. Proteins were extracted using an extraction buffer containing 20 mM HEPES (pH 6.8), 150 mM NaCl, 1 mM EDTA, 1 mM dithiothreitol, 0.5% Tween 20, 1 mM PMSF, and a protease inhibitor cocktail (Roche) and pulled down using GFP-trap agarose magnetic beads (Chromotek). Samples were subjected to LC-ESI-MS/MS analysis at the Clinical Proteomics Mass Spectrometry Facility, Karolinska Institute, Karolinska University Hospital, Science for Life Laboratory, Stockholm. Proteome Discoverer v. 1.4, including Sequest-Percolator, was used to search the *N. benthamiana* v044 database for protein identification, which was limited to a false discovery rate of 1%.

4.11 | Co-IP and Y2H assays

For Y2H, the vectors shown in Table S7 were transformed into *Saccharomyces cerevisiae* AH109 (Clontech). Transformations with empty vectors were used as negative controls. For co-IP assays, pGWB605-VlsPLA$_2^{WT}$ or pGWB605-VlsPLA$_2^{\Delta NLS1NLS2}$ was transiently co-expressed with pGWB614-NbVAMPA1 in *N. benthamiana* and pulled down as described above for the MS/MS assays. GFP-tagged proteins were detected using a B2 anti-GFP horseradish peroxidase-conjugated antibody (Santa Cruz Biotechnology), and HA-tagged proteases were detected using an anti-HA peroxidase-conjugated antibody (Sigma) according to the manufacturer's instructions.

4.12 | RNA sequencing and bioinformatics analysis

For the transcriptomic analysis of *V. longisporum* mycelia, the WT, *VlsPLA$_2$+*^{WT}, and *VlsPLA$_2$+*$^{\Delta CD}$ strains were grown in PDB (Difco) for 5 days at 20°C. For in planta transcriptomic analysis, *N. benthamiana* plants were agroinfiltrated with pGWB602-VlsPLA$_2^{WT}$ and pGWB602-VlsPLA$_2^{\Delta CD}$ as well as the empty vector (pGWB602) as described above. RNA strand-specific libraries were constructed using the TruSeq stranded mRNA library preparation kit with polyA selection (Illumina, Inc.) and sequenced using an Illumina NovaSeq 6000 at the SNP & SEQ Technology Platform, Science for Life Laboratory at Uppsala University, Sweden. The experiment was performed with four biological replicates.

Bioinformatic analysis was performed as follows. Reads were trimmed using bbduk v. 38.9 with default parameters (Bushnell, 2018). Successful cleaning and adapter removal were conducted using the fastqc v. 11.9 quality control tool (Andrews, 2010). *V. longisporum* reads were then mapped to the *V. longisporum* VL1 genome (accession GCA_001268145.1) using the splice-aware aligner STAR v. 2.7.9a with default parameters (Dobin et al., 2013). The *N. benthamiana* reads were mapped to the *N. benthamiana* v.5.1 transcriptome (http://sefapps02.qut.edu.au/benWeb/subpages/downloads.php) using the nonsplice-aware aligner bowtie2 v. 2.4.2 with default parameters (Langmead & Salzberg, 2012). The number of reads mapped to each gene was quantified using featureCounts v. 2.0.1 (Liao et al., 2014) considering only sense reads, and differential expression was determined with the DESeq2 R package v. 1.28.1 using a minimal threshold of $\log_2$(fold change) > 1 and false discovery rate adjusted p-value < 0.05 (Love et al., 2014). Data visualization was performed using the R pheatmap module.

For functional annotation, protein sequences were extracted from the genome and gene coordinate files of *N. benthamiana* and *V. longisporum* using GffRead v. 0.12.2, and additional domains were determined using default parameters (Pertea & Pertea, 2020). *V. longisporum* proteins were mapped to the PHI-base database v. 09-05-2022 with a minimum identity and query coverage of 80% (Urban et al., 2017).

More details on the experimental procedures can be found in Text S1.

ACKNOWLEDGEMENTS

This work was funded by the Swedish Research Council FORMAS (grant 942-2015-36), the Helge Axelsson Johnson Foundation, the Carl Tryggers Foundation (grant CTS 19:374), and the Department of Forest Mycology and Plant Pathology. We would like to thank Wageningen University for providing us with *N. benthamiana* Cf4 seeds, the Protein Expertise Platform for the cloning, expression, and purification of VlsPLA$_2$, and the Swedish Metabolomics Centre for lipidomic analysis at Umeå University. We would also like to thank the Clinical Proteomics Mass Spectrometry Facility at Karolinska Institute for MS/MS analysis and the SNP & SEQ Platform at the Science for Life Laboratory, Uppsala, for the RNA-seq analyses. We are also grateful to Anna Tornkvist for helping us with confocal microscopy and to Jerry Stålberg for the VlsPLA$_2$ protein structure prediction and analysis.

CONFLICT OF INTEREST STATEMENT

The authors declare that there are no conflicts of interest.

DATA AVAILABILITY STATEMENT

The transcriptomic data of this study (*V. longisporum* and *N. benthamiana* reads) were deposited in the European Nucleotide Archive database at www.ebi.ac.uk/ena/ under BioProject accession number PRJEB55988.

ORCID

Vahideh Rafiei https://orcid.org/0000-0003-0021-9734
Heriberto Vélëz https://orcid.org/0000-0003-3146-0555
Edoardo Piombo https://orcid.org/0000-0003-2830-1967
Mukesh Dubey https://orcid.org/0000-0001-7393-366X
Georgios Tzelepis https://orcid.org/0000-0001-6144-2185

REFERENCES

Aloulou, A., Ben Ali, Y., Bezzine, S., Gargouri, Y. & Gelb, M.H. (2012) Phospholipases: an overview. *Lipases and Phospholipases: Methods and Protocols*, 861, 63–85.

Andrews, S. (2010) FastQC: a quality control tool for high throughput sequence data. Available at: https://www.bioinformatics.babraham.ac.uk/projects/fastqc/ [Accessed 26th April 2023].

Beres, S.B., Sylva, G.L., Barbian, K.D., Lei, B., Hoff, J.S., Mammarella, N.D. et al. (2002) Genome sequence of a serotype M3 strain of group a *Streptococcus*: phage-encoded toxins, the high-virulence phenotype, and clone emergence. *Proceedings of the National Academy of Sciences of the United States of America*, 99, 10078–10083.

Berthelot, P., Attree, I., Plésiat, P., Chabert, J., de Bentzmann, S., Pozzetto, B. et al. (2003) Genotypic and phenotypic analysis of type III secretion system in a cohort of *Pseudomonas aeruginosa* bacteremia isolates: evidence for a possible association between O serotypes and exo genes. *Journal of Infectious Diseases*, 188, 512–518.

Boller, T. & Felix, G. (2009) A renaissance of elicitors: perception of microbe-associated molecular patterns and danger signals by pattern-recognition receptors. *Annual Review of Plant Biology*, 60, 379–406.

Bushnell, B. (2018) *BBTools: a suite of fast, multithreaded bioinformatics tools designed for analysis of DNA and RNA sequence data*. Berkeley, CA, USA: Joint Genome Institute. Available at: sourceforge.net/projects/bbmap/ [Accessed 26th April 2023].

Charova, S.N., Dölfors, F., Holmquist, L., Moschou, P.N., Dixelius, C. & Tzelepis, G. (2020) The RsRlpA effector is a protease inhibitor promoting *Rhizoctonia solani* virulence through suppression of the hypersensitive response. *International Journal of Molecular Sciences*, 21, 8070.

Collmer, A., LIndeberg, M., Petnicki-Ocwieja, T., Schneider, D.J. & Alfano, J.R. (2002) Genomic mining type III secretion system effectors in *Pseudomonas syringae* yields new picks for all TTSS prospectors. *Trends in Microbiology*, 10, 462–469.

Couto, D. & Zipfel, C. (2016) Regulation of pattern recognition receptor signalling in plants. *Nature Reviews Immunology*, 16, 537–552.

Crespo-Sempere, A., Lopez-Perez, M., Martinez-Culebras, P.V. & Gonzalez-Candelas, L. (2011) Development of a green fluorescent tagged strain of *Aspergillus carbonarius* to monitor fungal colonization in grapes. *International Journal of Food Microbiology*, 148, 135–140.

Depotter, J.R., Deketelaere, S., Inderbitzin, P., Tiedemann, A.V., Höfte, M., Subbarao, K.V. et al. (2016) *Verticillium longisporum*, the invisible threat to oilseed rape and other brassicaceous plant hosts. *Molecular Plant Pathology*, 17, 1004–1016.

Di Mattia, T., Wilhelm, L.P., Ikhlef, S., Wendling, C., Spehner, D., Nominé, Y. et al. (2018) Identification of MOSPD2, a novel scaffold for endoplasmic reticulum membrane contact sites. *EMBO Reports*, 19, e45453.

Dobin, A., Davis, C.A., Schlesinger, F., Drenkow, J., Zaleski, C., Jha, S. et al. (2013) STAR: Ultrafast universal RNA-seq aligner. *Bioinformatics*, 29, 15–21.

Dunker, S., Keunecke, H., Steinbach, P. & von Tiedemann, A. (2008) Impact of *Verticillium longisporum* on yield and morphology of winter oilseed rape (*Brassica napus*) in relation to systemic spread in the plant. *Journal of Phytopathology*, 156, 698–707.

Figueiredo, A., Monteiro, F. & Sebastiana, M. (2014) Subtilisin-like proteases in plant-pathogen recognition and immune priming: a perspective. *Frontiers in Plant Science*, 5, 739.

Fogelqvist, J., Tzelepis, G., Bejai, S., Ilback, J., Schwelm, A. & Dixelius, C. (2018) Analysis of the hybrid genomes of two field isolates of the soil-borne fungal species *Verticillium longisporum*. *BMC Genomics*, 19, 14.

Froidure, S., Canonne, J., Daniel, X., Jauneau, A., Brière, C., Roby, D. et al. (2010) AtsPLA2-alpha nuclear relocalization by the *Arabidopsis* transcription factor AtMYB30 leads to repression of the plant defense response. *Proceedings of the National Academy of Sciences of the United States of America*, 107, 15281–15286.

Ghannoum, M.A. (2000) Potential role of phospholipases in virulence and fungal pathogenesis. *Clinical Microbiogical Reviews*, 13, 122–143.

Giraldo, M.C. & Valent, B. (2013) Filamentous plant pathogen effectors in action. *Nature Reviews Microbiology*, 11, 800–814.

Grewal, S., Morrison, E.E., Ponnambalam, S. & Walker, J.H. (2002) Nuclear localisation of cytosolic phospholipase A2-α in the EA.hy.926 human endothelial cell line is proliferation dependent and modulated by phosphorylation. *Journal of Cell Science*, 115, 4533–4543.

Hong, Y., Zhao, J., Guo, L., Kim, S.C., Deng, X., Wang, G. et al. (2016) Plant phospholipases D and C and their diverse functions in stress responses. *Progress in Lipid Research*, 62, 55–74.

Inderbitzin, P., Bostock, R.M., Davis, R.M., Usaml, T., Platt, H.W. & Subbarao, K.V. (2011) Phylogenetics and taxonomy of the fungal vascular wilt pathogen *Verticillium*, with the descriptions of five new species. *PLoS One*, 6, e28341.

Jones, J.D.G. & Dangl, J.L. (2006) The plant immune system. *Nature*, 444, 323–329.

Joosten, M.H.A.J., Vogelsang, R., Cozijnsen, T.J., VErberne, M.C. & de Wit, P.J.G.M. (1997) The biotrophic fungus *Cladosporium fulvum* circumvents Cf-4-mediated resistance by producing unstable AVR4 elicitors. *The Plant Cell*, 9, 367–379.

Kim, H., O'Connell, R., Maekawa-Yoshikawa, M., Uemura, T., Neumann, U. & Schulze-Lefert, P. (2014) The powdery mildew resistance protein RPW8.2 is carried on VAMP721/722 vesicles to the extrahaustorial membrane of haustorial complexes. *The Plant Journal*, 79, 835–847.

Kumar, S., Stecher, G., Li, M., Knyaz, C. & Tamura, K. (2018) MEGA X: molecular evolutionary genetics analysis across computing platforms. *Molecular Biology and Evolution*, 35, 1547–1549.

Langmead, B. & Salzberg, S.L. (2012) Fast gapped-read alignment with bowtie 2. *Nature Methods*, 9, 357–359.

Letunic, I., Doerks, T. & Bork, P. (2009) SMART 6: recent updates and new developments. *Nucleic Acids Research*, 37, D229–D232.

Lev, S., Ben Halevy, D., Peretti, D. & Dahan, N. (2008) The VAP protein family: from cellular functions to motor neuron disease. *Trends in Cell Biology*, 18, 282–290.

Liao, Y., Smyth, G.K. & Shi, W. (2014) FeatureCounts: an efficient general purpose program for assigning sequence reads to genomic features. *Bioinformatics*, 30, 923–930.

Livak, K.J. & Schmittgen, T.D. (2001) Analysis of relative gene expression data using real-time quantitative PCR and the $2(T^{(-\Delta\Delta C(t))})$ method. *Methods*, 25, 402–408.

Lo Presti, L., Lanver, D., Schweizer, G., Tanaka, S., Liang, L., Tollot, M. et al. (2015) Fungal effectors and plant susceptibility. *Annual Reviews of Plant Biology*, 66, 513–545.

Love, M.I., Anders, S. & Huber, W. (2014) Differential analysis of count data—the DESeq2 package. *Genome Biology*, 15, 550.

Matoba, Y., Katsube, Y. & Sugiyama, M. (2002) The crystal structure of prokaryotic phospholipase A_2. *Journal of Biological Chemistry*, 277, 20059–20069.

Murakami, M. & Kudo, I. (2004) Secretory phospholipase A_2. *Biological and Pharmaceutical Bulletin*, 27, 1158–1164.

Nakamura, Y. (2017) Plant phospholipid diversity: emerging functions in metabolism and protein-lipid interactions. *Trends in Plant Science*, 22, 1027–1040.

Nygren, H., Seppänen-Laakso, T., Castillo, S., Hyötyläinen, T. & Orešič, M. (2011) Liquid chromatography-mass spectrometry (LC-MS)-based lipidomics for studies of body fluids and tissues. *Methods in Molecular Biology*, 708, 247–257.

Pertea, G. & Pertea, M. (2020) GFF utilities: GffRead and GffCompare. *F1000 Research*, 9, ISCB Comm J-304.

Petersen, N.H.T., Joensen, J., McKinney, L.V., Brodersen, P., Petersen, M., Hofius, D. et al. (2009) Identification of proteins interacting with *Arabidopsis* ACD11. *Plant Physiology*, 166, 661–666.

Peters-Golden, M., Song, K., Marshall, T. & Brock, T. (1996) Translocation of cytosolic phospholipase A_2 to the nuclear

envelope elicits topographically localized phospholipid hydrolysis. *Biochemical Journal*, 318, 797–803.
Pireyre, M. & Burow, M. (2015) Regulation of MYB and bHLH transcription factors: a glance at the protein level. *Molecular Plant*, 8, 378–388.
Rafiei, V., Najafi, Y., Vélëz, H. & Tzelepis, G. (2022) Investigating the role of a putative endolysin-like candidate effector protein in *Verticillium longisporum* virulence. *Biochemical and Biophysical Research Communications*, 629, 6–11.
Rafiei, V., Ruffino, A., Persson-Hoden, K., Tornkvist, A., Mozuraitis, R., Dubey, M. et al. (2022) A *Verticillium longisporum* pleiotropic drug transporter determines tolerance to the plant host beta-pinene monoterpene. *Molecular Plant Pathology*, 23, 291–303.
Rafiei, V., Vélëz, H. & Tzelepis, G. (2021) The role of glycoside hydrolases in phytopathogenic fungi and oomycetes virulence. *International Journal of Molecular Sciences*, 22, 9359.
Rowland, O., Ludwig, A.A., Merrick, C.J., Baillieul, F., Tracy, F.E., Durrant, W.E. et al. (2005) Functional analysis of Avr9/Cf-9 rapidly elicited genes identifies a protein kinase, ACIK1, that is essential for full Cf-9-dependent disease resistance in tomato. *The Plant Cell*, 17, 295–310.
Santhanam, P. & Thomma, B.P. (2013) *Verticillium dahliae* Sge1 differentially regulates expression of candidate effector genes. *Molecular Plant-Microbe Interactions*, 26, 249–256.
Santos, M.F., Rappa, G., Karbanová, J., Kurth, T., Corbeil, D. & Lorico, A. (2018) VAMP-associated protein-a and oxysterol-binding protein-related protein 3 promote the entry of late endosomes into the nucleoplasmic reticulum. *Journal of Biological Chemistry*, 293, 13834–13848.
Saravanan, R.S., Slabaugh, E., Singh, V.R., Lapidus, L.J., Haas, T. & Brandizzi, F. (2009) The targeting of the oxysterol-binding protein ORP3a to the endoplasmic reticulum relies on the plant VAP33 homolog PVA12. *The Plant Journal*, 58, 817–830.
Sitkiewicz, I., Stockbauer, K.E. & Musser, J.M. (2007) Secreted bacterial phospholipase A2 enzymes: better living through phospholipolysis. *Trends in Microbiology*, 15, 63–69.
Sperschneider, J., Catanzariti, A.M., DeBoer, K., Petre, B., Gardiner, D.M., Singh, K.B. et al. (2017) LOCALIZER: subcellular localization prediction of both plant and effector proteins in the plant cell. *Scientific Reports*, 7, 44598.
Sperschneider, J., Dodds, P.N., Singh, K.B. & Taylor, J.M. (2018) ApoplastP: prediction of effectors and plant proteins in the apoplast using machine learning. *New Phytologist*, 217, 1764–1778.
Tian, L., Yu, J., Wang, Y. & Tian, C. (2017) The C2H2 transcription factor VdMsn2 controls hyphal growth, microsclerotia formation, and virulence of *Verticillium dahliae*. *Fungal Biology*, 121, 1001–1010.
Tzelepis, G., Bejai, S., Sattar, M.N., Schwelm, A., Ilback, J., Fogelqvist, J. et al. (2017) Detection of *Verticillium* species in Swedish soils using real-time PCR. *Archives of Microbiology*, 199, 1383–1389.
Urban, M., Cuzick, A., Rutherford, K., Irvine, A., Pedro, H., Pant, R. et al. (2017) PHI-base: a new interface and further additions for the multi-species pathogen-host interactions database. *Nucleic Acids Research*, 45, 604–610.
Utermark, J. & Karlovsky, P. (2008) Genetic transformation of filamentous fungi by *Agrobacterium tumefaciens*. *Protocol Exchange*. Available at: http://www.nature.com/protocolexchange/protocols/427 [Accessed 26th April 2023].
van den Burg, H.A., Tsitsigiannis, D.I., Rowland, O., Lo, J., Rallapalli, G., Maclean, D. et al. (2008) The F-box protein ACRE189/ACIF1 regulates cell death and defense responses activated during pathogen recognition in tobacco and tomato. *The Plant Cell*, 20, 697–719.
Waterhouse, A., Bertoni, M., Bienert, S., Studer, G., Tauriello, G., Gumienny, R. et al. (2018) SWISS-MODEL: homology modelling of protein structures and complexes. *Nucleic Acids Research*, 46, W296–W303.
Zhang, T., Zhao, Y.L., Zhao, J.H., Wang, S., Jin, Y., Chen, Z.Q. et al. (2016) Cotton plants export microRNAs to inhibit virulence gene expression in a fungal pathogen. *Nature Plants*, 2, 16153.
Zhao, J. (2015) Phospholipase D and phosphatidic acid in plant defence response: from protein-protein and lipid-protein interactions to hormone signalling. *Journal of Experimental Botany*, 66, 1721–1736.

SUPPORTING INFORMATION

Additional supporting information can be found online in the Supporting Information section at the end of this article.

How to cite this article: Rafiei, V., Vélëz, H., Piombo, E., Dubey, M. & Tzelepis, G. (2023) *Verticillium longisporum* phospholipase $VlsPLA_2$ is a virulence factor that targets host nuclei and modulates plant immunity. *Molecular Plant Pathology*, 24, 1078–1092. Available from: https://doi.org/10.1111/mpp.13352